Effect of focus position on informational properties of acoustic emission generated by laser–material interactions

Bordatchev, Evgueni V.; Nikumb, Suwas K

Publisher's version / Version de l'éditeur:
https://doi.org/10.1016/j.apsusc.2006.01.047
Applied Surface Science, 253, 3, pp. 1122-1129, 2006-02-28

Effect of Focus Position on Informational Properties of Acoustic Emission Generated by Laser-Material interactions

Evgueni V. Bordatchev and Suwas K. Nikumb

Integrated Manufacturing Technologies Institute
National Research Council of Canada
London, Ontario, N6G 4X8, Canada

October 2005

Submitted to: Applied Surface Science

For correspondence:
Evgueni V. Bordatchev, Ph.D., D.Sc., Prof.
Integrated Manufacturing Technologies Institute
National Research Council of Canada
800 Collip Circle, London, ON, Canada, N6G 4X8
Tel: (519) 430-7107
Fax: (519) 430-7064
E-mail: evgueni.bordatchev@nrc-cnrc.gc.ca

PACS codes:

52.38.Mf Laser ablation
42.62.Cf Industrial applications
52.35.Tc Shock waves and discontinuities
43.35.Kp Plasma acoustics
43.60.Cg Statistical properties of signals and noise
52.35.Dm Sound waves
05.45.Tp Time series analysis
43.20.Fn Scattering of acoustic waves
43.60.+d Acoustic signal processing
43.60.Lq Displays, pattern recognition, learning machines, adaptive processing

Effect of Focus Position on Informational Properties of Acoustic Emission Generated by Laser-Material interactions

Evgueni V. Bordatchev* **and Suwas K. Nikumb**

Integrated Manufacturing Technologies Institute, National Research Council of Canada
London, Ontario, N6G 4X8, Canada

To achieve desired accuracy, precision and surface roughness during laser material removal process, monitoring and control of the process parameters related to laser, optics, workpiece material and its motion are required. Focus position, defined as a gap between the focusing lens and the surface of the sample workpiece, is one of the most critical process parameters, which determines the projection of the intensity of the laser beam on the surface to be ablated and therefore directly affects volume and geometry of the material removed and there by machining quality. In this paper, acoustic emission (AE) generated by laser-material interactions was statistically analyzed with respect to the variations in the focus position. The study involved on-line measurements of the AE signal from the laser-material interaction zone as a function of the focus position and the width of the machined trenches. Several basic statistical parameters, e.g. average amplitude, variance and power spectrum density were analyzed to select distinct informational parameters. Pattern recognition analysis of three informational parameters based on variances within frequency diapasons of 20 – 180 kHz, 180 – 300 kHz, and 300 – 500 kHz was used for reliable classification of the focus position and width of the machined trenches. The results provide important information for future development of on-line monitoring and control systems for laser-material removal process.

Keywords: laser-material interaction; focus position; acoustic emission; statistic analysis; informational properties; pattern recognition; on-line monitoring

* Corresponding author. Tel.: 1-519-430-7107; fax: 1-519-430-7064; e-mail: evgueni.bordatchev@nrc.ca

1. INTRODUCTION

The significance of the focus position, referred as the location of the focal spot (focus above, focus below and focus on the surface of the sample), was first indicated in laser welding and laser cutting technologies, where variations in the surface profile can be within several millimeters, and therefore, focus position control systems are critical for achieving desired accuracy, precision and surface quality [1-5]. For laser welding, the penetration depth of the welds is maximized at the focal position of –0.5 mm (negative sign indicates that focus below the surface), and the depth varies as the focal position below or above due to the lower laser intensity levels or out of focus conditions [3]. The laser micromachining applications do not experience such large variations in surface geometry [6]. However, in the ultra-precision laser-material removal processes, focusing of the laser beam and location of the focal plane with respect to the ablated surface are very important factors that significantly affect the energy transfer efficiency and corresponding depth, width and volume of the material removed during laser ablation, ultimately contributing to the accuracy, precision and surface quality of the laser machined parts [7-9]. The performance of the laser-material removal process relies on many process parameters, starting with the laser beam characteristics, such as wavelength, pulse energy, repetition rate, beam intensity profile, the workpiece material properties and the overlap between two consecutive laser pulses. In addition, the location of the focal plane with respect to the ablated surface, the diameter of the focal spot and beam waist determine the impinging laser beam energy into the laser-material interaction zone due to the changes in its diameter and spatial energy distribution (beam density) during propagation. In numerous studies related to the dynamics of the laser-material interactions and effect of different aforementioned process parameters [1, 10-16], often, considerations related to the location of the focal plane and

associated intensity distribution are not taken in to account. It is generally a common practice to focus laser beam slightly below the surface.

In this paper, the effect of the focus position, referred to as a gap between the focusing lens and the laser ablated surface, on the laser-material removal process is studied utilizing the analysis of AE generated by laser-material interactions. On-line measurement, statistical and pattern recognition analysis of the AE signal from the laser-material interaction zone with respect to variations in the focus position and width of the machined trenches are presented.

2. THEORETICAL BACKGROUND, EXPERIMENTAL SET-UP AND PROCEDURE

The laser beam irradiance related characteristics, such as laser power, pulse energy, intensity, and laser-material interaction time are the key parameters that define the volume of material removed. The volume of the vaporized material as a function of the laser beam intensity at the melt surface, I, and the laser pulse duration, τ, is calculated by considering the following energy balance (Stefan condition) at the vapour-liquid and liquid-solid interfaces [17], respectively:

$$\rho_\ell L_v \dot{S}_v = AI + k_\ell \left(\frac{T_s - T_m}{(\dot{S}_m - \dot{S}_v)\tau} \right) \tag{1}$$

$$\rho_\ell L_m \dot{S}_m = k_\ell \left(\frac{T_s - T_m}{(\dot{S}_m - \dot{S}_v)\tau} \right) - k_s \left(\frac{T_m - T_\infty}{2\sqrt{\alpha\tau}} \right) \tag{2}$$

where A is the absorptivity of the melt surface; k_ℓ and ρ_ℓ are the normal conductivity and density of the ablated material at the melting temperature, respectively; L_v and L_m are the latent constants of boiling and melting, respectively; α is the thermal diffusivity; k_s is the thermal

conductivity, and $\dot{S}_m$ is the solid-liquid interface velocity.

If the pulse duration, τ, is a stable parameter with small variations for any given laser system, the laser beam intensity at the melt surface, I, is defined by the focus position with respect to the surface of ablated material. Different focus position corresponds to the different laser beam intensity due to the fact that a TEM00 mode laser beam with input diameter d and wavelength λ transmitted through a thin lens with focal length f propagates along axial distance Z its actual radius w changes from the beam waist radius w_0 [18]:

$$w(Z) = w_0\sqrt{1+(Z/Z_0)^2}\text{, where } w_0 \approx 2\frac{\lambda f}{\pi d},\ Z_0 = \frac{\pi w_0^2}{\lambda} \tag{3}$$

Therefore, the optical intensity of the laser beam also changes as a function of the axial, Z, and radial, $r = \sqrt{x^2+y^2}$, coordinates [19]:

$$I(r,Z) = \frac{2P}{\pi w^2(Z)}\exp\left(-\frac{2r^2}{w^2(Z)}\right) \tag{4}$$

where P is the total optical power. The geometry and intensity of the Gaussian laser beam shown on Figure 1.

['Insert figure 1 about here']

In laser micromachining technology, Z coordinate is associated with one of the most critical process parameter - focus position, h (see Figure 1), which is a set-up parameter in industrial applications. As it can be seen from Equation 4, changes in the focus position correspond to the actual optical intensity and power above the laser ablation threshold delivered onto the ablated surface. Therefore, the focus position affects the dynamics of the laser-material

removal process and the geometry of the ablated surface. This effect and its correlation with AE is an objective of this research.

Figure 2 shows the schematics of the experimental set-up for the AE measurements and procedure of experiments. A thick brass foil with a thickness of 152 μm was used in this study. The laser ablation experiments were carried out using a Q-switched diode pumped solid state Nd:YVO4 laser with an appropriate beam delivery system and a three-axis positioning system. The laser has a pulse width of 12 ns with a wavelength of 1064 nm for TEM00 mode. A beam delivery system with a combination of a beam expander and x10 focusing objective was used to focus the laser beam on the workpiece surface. The focusing objective has a nominal focus position of 15 mm, effective focal length of 20 mm and a calculated focal spot diameter of 6 μm. The motion system consisted of a granite base fitted with precision translation stages with air bearings and linear motors for X and Y movements and had a positioning accuracy in the order of 0.5 μm in the X and Y axis. Both the laser and the motion system were controlled and synchronized in time and space.

['Insert figure 2 about here']

During experiments, the focus position was varied from 14.710 mm to 15.385 mm with a step increment of 75 μm. Several trenches with a length of 0.5 mm were machined on the brass plate by moving the sample at a feed rate of 2 mm/s. The laser pulses at a frequency of 10 kHz and pulse energy of 0.055 μJ were applied. An optical microscope "Olympus" (model PMG3), VisionGauge software and a WYKO surface profilometer were used to measure the width of the machined trenches within an accuracy of 0.1 μm.

AE was measured using a high-fidelity acoustic emission transducer SE1000-HI (Dunegan Engineering Consultants Inc.). The sensor having a frequency bandwidth of up to 500 kHz, a dynamic range of 74 dB, a diameter of 20 mm and a height of 22 mm, was directly placed in contact with the top surface of the workpiece sample 30 mm away from the laser-material interaction zone. The data, related to AE, was recorded using a digital oscilloscope (Tektronix TDS 724C, maximum sampling frequency of 500 MHz). The continuous waveform from the sensor, triggered by the first laser pulse and digitized in time and amplitude, produced digital time series. Each time series was recorded for 130 ms duration, giving 130000 data points with a sampling period of 1 μs (sampling frequency of 1 MHz). The data were truncated for first 30 ms to expel non-stationary behavior of the laser-material interactions at the beginning of travel motions. Afterwards, the remaining data (100 ms long) were filtered out below 10 kHz to remove electro-mechanical disturbances from the motion system and were statistically analyzed using MATLABTM (The MathWorks, Inc) signal processing routines, such as mean, average amplitude, standard deviation, variance, Fast Fourier Transformation (FFT) and power spectrum [20], and methods of the pattern recognition analysis [21].

Before calculating a power spectrum, the original time interval, $\tilde{\mathbf{x}} = [\tilde{x}_i]$, $i = 1...100000$, was tabulated in terms of normalized (standardized) variable [20]

$$z_i = (\tilde{x}_i - \mu)/\sigma \tag{5}$$

where μ and σ are the mean value and standard deviation of $\tilde{\mathbf{x}}$ respectively. This mathematical procedure produces dimensionless time series with a zero mean value, $mean(\mathbf{z}) = 0$, and a unit variance, $\mathrm{var}(\mathbf{z}) = 1$. Due to this normalization procedure all data series have an equal unit energy represented by $\mathrm{var}(\mathbf{z}) = 1$. Therefore, the unit of calculated power spectrum densities is 1/Hz. This mathematical procedure was implemented to exclude unknown

effect of signal amplitudes with respect to laser ablation process that can be different for different lasers. The goal of our study is to propose and explore statistical signatures of AE generated by laser-material interactions independent of the laser used and location of the AE transducer. This approach is based on the analysis of the distribution of frequency components within the normalized power spectrum density. This distribution was represented by three variances, V_1, V_2, and V_3, where $V_1 + V_2 + V_3 = 1$, in different frequency diapasons depended on signatures in the experimental results. The selected variances were adopted as informational parameters and were used for further studies using the linear-discriminant-based pattern recognition analysis [21] involving the focus position and width of the machined trenches.

It is necessary to note that this study is a logical continuation of the authors' previous research [22] investigated the spectral characteristics of the AE signal caused by a single laser pulse and the effect of variation in laser pulse energy concluding that the AE signal generated by a single laser pulse has non-stationary random properties and time-varying statistical and spectral signatures.

3. ANALYSIS, RESULTS AND DISCUSSION

Figure 3 shows examples of the measured and calculated parameters, such as trench width, original (measured) AE signal and power spectrum density, corresponding to a set of focus position values {14.71, 14.86, 15.01, 15.16, 15.31} mm. Initially, the trench width was analyzed with respect to the focus position (see Figure 3a) and results are presented in Figure 4. The trench width decreases from 40.1 μm initially while the focus position increases from 14.71 mm until the width reaches a noticeable minimum of 22.2 μm corresponding to the manufacturer-suggested nominal focus position of 15.0 mm. After reaching its minimum, the trench width climbs up again up to 44.1 mm for a focus position of 15.385 mm. These results

correlate with published experimental results [7-9] and with our understanding of the relationship between the geometry of the Gaussian laser beam and the focus position presented in Figure 1. A wide trench width corresponds to a wider laser spot diameter when focus is above or below of the ablated surface, and a minimal trench width is a result of focusing the laser beam on the surface.

['Insert figure 3 about here']

['Insert figure 4 about here']

Any change in the focal position with respect to the ablated surface causes a change at the interface between the laser beam profile and the sample surface, and therefore, a change in the dynamics of the laser-material interactions, which eventually translates in to the signatures of AE generated by the laser-material removal process. Knowing a specific type of AE signal as a random process (non-stationary/stationary, non-ergodic/ergodic) is very important in choosing a proper and most effective signal processing approach for statistical analysis. For this reason, a moving average of the amplitude and variance of the measured AE signals shown in Figure 3b was calculated over the time period of 100 ms corresponding to the travel distance of 0.2 mm, focus position of 15.010 mm, and the results are shown in Figure 5. These results confirm that the AE signal significantly changes over time during laser-material interactions and hence, over the distance of the laser cutting. For example, a variation of the amplitude is within 6.46 mV, i.e. a 66.2% with respect to a mean value of the AE signal amplitude of 9.76 mV. The variance has a similar behavior with variations of 3.43 mV^2 that corresponds to 111.2 % with respect to a

mean value of the AE signal variance of 3.08 mV^2.

['Insert figure 5 about here']

The power spectrum densities of the AE signals (see Figure 3c) significantly change the frequency distribution of the signal energy with respect to the focus position. The power spectrum densities for the focal positions below 14.710 mm and above 15.310 mm, the ablated surface, show even distribution of the AE signal energy within 100 – 450 kHz diapason. With changes in the focus position, this distribution can be classified into two separate frequency diapasons, 20 – 180 kHz and 300 – 500 kHz with highest amplitudes for the focus positions lie between 14.860 – 15.160 mm. Completely different behavior was observed for a frequency diapason between 50 – 70 kHz, where the amplitude constantly increases over the increase in the focus position and does not have any extreme corresponding to the minimum width of the machined trench.

The above results support our understanding of the AE signal as a non-stationary and non-ergodic random process generated by the non-stationary and non-linear laser-material interactions. Therefore, for analysis, monitoring and diagnostics of the laser-material removal process, the methods of the non-linear statistical, pattern recognition and multi-variable analysis are required.

Considering the observations mentioned above, the calculated power spectrum densities (see Figure 3c), three frequency diapasons were selected, 20 – 180 kHz, 180 – 300 kHz, and 300 – 500 kHz, and variances of the signal within each diapason were calculated as

$$V_1 = \int_{20\,kHz}^{180\,kHz} S_{ZZ}(f)df\,, \quad V_2 = \int_{180\,kHz}^{300\,kHz} S_{ZZ}(f)df\,, \quad V_1 = \int_{300\,kHz}^{500\,kHz} S_{ZZ}(f)df\,, \tag{5}$$

where

$$V_1 + V_2 + V_3 = \int_{20\,kHz}^{500\,kHz} S_{ZZ}(f)df = 1 \tag{6}$$

where $S_{ZZ}(f)$ is the normalized power spectrum density of the AE signal, 1/Hz, and f is the frequency, Hz. These variances, V_1, V_2, and V_3, were selected as informational parameters for further statistical and pattern recognition analysis.

The relationships between the focus position and variances, V_1, V_2, and V_3, shown in Figure 4, indicate that there exists no obvious correlation between these parameters. Only the trench width has an extreme (minimum) with respect to the focus position, which corresponds to the optimal focus position with a minimum trench width. In practice, this study is called a "line test", when several lines are machined with different focus positions in order to find an optimal focus position corresponding to a trench with a minimum width. This test requires several off-line measurements of the trench geometry that may involve errors caused by a "human factor." Any of V_1, V_2, and V_3 parameters does not have an extreme corresponding to the minimal trench width and/or optimal focus position. On the other hand, all these parameters have distinctly different behavior in relation to the trench width and/or optimal focus position. Therefore, the pattern recognition analysis [21] was proposed for further analysis.

In general, pattern recognition analysis is based on the linear discriminant theory and allows separation of data within n-dimensional informational space into clusters with specific and unique properties. Decisions for the separation obey strict mathematical rules called linear decision functions, which were calculated using Bayesian classifiers (Bayes' decision functions), and do not involve human decisions. Informational parameters, V_1, V_2, V_3, cannot be used individually for proper estimation and prediction of the laser pulse energy because they are

overlapped across the focus position (see Figure 4). Therefore, in order to choose the best combinations of informational parameters (from the statistical point of view), a multi-variable approach was selected, and four different informational spaces, $\{V_1,V_2,V_3\}$, $\{V_1,V_2\}$, $\{V_1,V_3\}$, $\{V_2,V_3\}$, were analyzed and compared. The ISODATA algorithm [21] was used for automatic data separation with respect to the set of the focus position values {14.710, 14.785, 14.860, 14.935, 15.010, 15.085, 15.160, 15.235, 15.310, 15.385} mm. In theory [21], each Bayes decision function is a function of minimum-distance pattern classifier. This means that distance, $d_i(\cdot)$, estimates a geometrical difference between an analyzed point and the center of the i^{th} cluster. Therefore the minimum, $\min(d_i(\cdot),\ i=1...10)$, indicates a cluster to which the analyzed point with coordinates $\{V_1,V_2,V_3\}$ belongs.

Figure 6 shows the Bayesian classification of informational parameters V_1, V_2 and V_3 within three information spaces $\{V_1,V_2\}$, $\{V_1,V_3\}$, and $\{V_2,V_3\}$ with respect to the focus position. These 2D informational spaces are the projections of 3D informational space $\{V_1,V_2,V_3\}$ onto corresponding planes. Figure 6 also illustrates the separating lines as the linear boundaries between clusters. The results of the pattern recognition analysis (see Figure 6) indicate that all combinations of informational parameters have similar trends and signatures, e.g. clusters {14.710, 14.785} mm, when the focal plane placed deeply below the surface, located very close to each other and therefore have a lower quality of cluster separation. Also, a general allocation of clusters within each information space has a similar inter-location in view of a two-loops (similar to a number "8") structure. The largest loop (bottom part of the number "8") is constantly represented by the inter-location of the clusters {14.785, 14.860, 14.935, 15.010, 15.235, 15.085, 15.310, 15.385} mm, and the small loop (top part of the number "8") is always a

combination of clusters with a focus position of {15.085, 15.160, 15.235} mm. In addition, the clusters {15.085, 15.235} mm are also located very close to each other with a low quality of separation due to the overlapping of these clusters and represent a "neck" of the number "8". All of these observations show a significant difference in the quality of the laser-material removal process when focal plane is placed above or below the ablated surface, and therefore it may be taken into consideration for more accurate and realistic mathematical modelling of the laser ablation process.

['Insert figure 6 about here']

4. SUMMARY AND CONCLUSIONS

This work presents a systematic study of AE generated by the laser-material interaction and focuses on the effect of the focus position on informational properties of the measured AE signals. During the laser ablation experiments, several trenches were machined and AE signal was simultaneously measured for different focus positions varied from 14.710 mm, when focus was below the surface, to 15.385 mm, when focus was above the surface, with a step increment of 75 μm. Supported by theoretical considerations, it was experimentally found that the width of machined trenches depends on the laser beam's geometric profile, focal position and focus position with respect to ablated surface, where minimal trench width corresponds to the focusing of the laser beam on the ablated surface. However, basic statistical parameters of measured AE signals, such as averaged amplitude, variance and power spectrum density, do not have any extremes and do not linearly correlate with the variations in the focus position, beam profile, and width of the machined trenches. In addition, it was found that amplitude-frequency distribution

within power spectrum densities significantly changes in coordination with variations of the focus position. Therefore, three informational parameters based on variances within frequency diapasons of 20 – 180 kHz, 180 – 300 kHz, and 300 – 500 kHz were proposed and analyzed using pattern recognition analysis. Following most essential conclusions can be drawn from these studies:

1. Acoustic emission generated by the laser ablation process has non-stationary random properties and time-varying statistical and spectral signatures and represent non-stationary character of the laser-material interactions.
2. The focus position, as an important parameter in the laser-material interactions, changes the dynamics and geometric profile of the machined surface and also the statistical properties of measured AE signal. These changes can be recognized through variances within frequency diapasons of 20 – 180 kHz, 180 – 300 kHz, and 300 – 500 kHz, as informational parameters.
3. Pattern recognition analysis of suggested informational parameters provides reliable statistical classification of actual focus position and can be used in diagnostic and control systems in laser processing technologies.

ACKNOWLEDGMENTS

Authors thank Mr. Mahmud-Ul Islam, Director, Production Technology Research, for his continued support in this work. The authors also appreciate the assistance of Matthew Shiu for his help in conducting laser machining experiments and Raj Vatsya for discussion and comments.

REFERENCES

1. *LIA Handbook of Laser Materials Processing*, Editor in Chief: J.F. Ready (Laser Institute of

America, Orlando, FL: Magnolia Publishing, USA, 2001).

2. C.L. Caristan, *Laser Cutting, Guide for Manufacturing* (Society of Manufacturing Engineers, Dearborn, MI, USA, 2003).
3. H.K. Tönshoff, A. Ostendorf, and W. Specker, "Quality Assurance of Laser Welding Process by Adaptive Close-Loop Process Control," in Proceedings of the International Congress on Applications of Lasers and Electro-Optics (Laser Institute of America, Orlando, FL, 2000), Vol. 89, Section E, pp. 252-261.
4. S.Q. Xie, Y.L. Tu, A. Shaw, and Z.C. Duan, "A Fussy Integral Sliding Mode Control Algorithm for High-Speed Laser Beam Focus Tracking Control," International Journal of Advanced Manufacturing Technology, **20**, 296-302 (2002).
5. M.D.T. Fox, P. French, C. Peters, D.P. Hand, and J.D.C. Jones, "Applications of Optical Sensing for Laser Cutting and Drilling," Applied Optics, 41, **24**, 4988-4995 (2002).
6. *Micromachining of Engineering Materials*, edited by J. McGeough (Marcel Dekker, New York, USA, 2002).
7. M. El-Bandrawy and M. C. Gupta, "Femtosecond Laser Micromachining of Silicon for MEMS," Proceedings of SPIE, **4977**, 219-225 (2003).
8. M. Nantel, K. Sue-Chu-Lam, and D. Grozdanovski, "New Autofocusing System for Laser Micromachining," Proceedings of SPIE, **4876**, 582-592 (2003).
9. T. Otani, L. Herbst, M. Heglin, S.V. Govorkov, and A.O. Wiessner, "Microdrilling and Micromachining with Diode-Pumped Solid-State Lasers," Applied Physics A, Materials Science and Processing, **79**, 1335-1339 (2004).
10. B.N. Chichkov, C. Momma, S. Nolte, F. von Alvensleben, and A. Tunnermann, "Femtosecond, picosecond and nanosecond laser ablation of solids," Appl. Phys. A **63**, 109-

115 (1996).

11. S. Nolte, C. Momma, H. Jacobs, A. Tunnermann, B.N. Chichkov, B. Wellegehausen, and H. Welling, "Ablation of metals by ultrashort laser pulses," J. Opt. Soc. Am. B **14** 2716-2722 (1997)
12. S.R. Vatsya, E.V. Bordatchev, and S.K. Nikumb, "Geometrical Modeling of Surface Profile Formation during Laser Ablation of Materials," Journal of Applied Physics, **93**(12), 9753-9759 (2003).
13. S.V. Govorkov, M. Scaggs, and H. Theoharidis, "High resolution microfabrication of hard materials with diode-pumped solid state (DPSS) UV laser," in Proceedings of the 20th International Congress on Applications of Lasers and Electro Optics (ICALEO) (Laser Institute America, Orlando, FL, USA, 2001), pp. 1620-1630.
14. J.J. Chang, B.E. Warner, E.P. Dragon, and M.W. Martinez, "Precision micromachining with pulsed green lasers," J. of Laser Applications, **10**(6), 285-291 (1998).
15. P. Di Pietro, Y.L Yao, and A. Jeromin, "Quality optimisation for laser machining under transient conditions," J of Materials Processing Technology, 97, 158-167 (2000).
16. E.V. Bordatchev and S.K. Nikumb, "An Experimental Study and Statistical Analysis of the Effect of Laser Pulse Energy on the Geometric Quality during Laser Precision Machining," Machining Science and Technology: An International Journal, **7**(1), 83-104 (2003).
17. S. Sankaranorayanan, H. Emminger, and A. Kar, "Energy Loss in the Plasma during Laser Drilling," Journal of Physics D: Applied Physics, **32**, 1605-1611 (1999).
18. B.A. Saleh and M.C. Teich, *Fundamentals of Photonics* (John Willey & Sons, Inc., New York, 1991, Ch. 3).
19. Yariv, A., Optical Electronics in Modern Communications, Oxford University Press, New

York, 1997, pp. 50-56

20. J.S. Bendat and A.G. Piersol, *Engineering Applications of Correlation and Spectral Analysis* (John Wiley & Sons, New York, 1993).
21. J.T. Tou and R.C. Gonzalez, *Pattern recognition principles* (Addison-Wesley, Reading, MS, 1974).
22. E.V. Bordatchev and S.K. Nikumb, "Informational Properties of Surface Acoustic Waves Generated by Laser-Material Interactions during Laser Precision Machining," Measurement Science and Technology Journal, **13**(6), 836-845 (2002).

LIST of TABLES

Table 1. Experimental parameters.

Experimental parameters Table 1.

focus position, *mm*	trench width, *μm*	variance within 20-180 *kHz*, dimensionless	variance within 180-300 *kHz*, dimensionless	variance within 300-500 *kHz*, dimensionless
14.710	40.1	0.174	0.145	0.681
14.785	39.2	0.191	0.144	0.666
14.860	36.7	0.202	0.089	0.709
14.935	32.1	0.202	0.066	0.732
15.010	22.2	0.259	0.086	0.656
15.085	27.1	0.263	0.112	0.625
15.160	33.5	0.283	0.079	0.638
15.235	37.8	0.267	0.105	0.628
15.310	41.2	0.212	0.130	0.658
15.385	44.1	0.139	0.128	0.733

LIST of Figure Captions

Figure 1. Geometry and intensity of the Gaussian laser beam.

Figure 2. Schematics of the experiment.

Figure 3. Examples of experimental data.

Figure 4. The relationships between the focus position, trench width and variances V_1, V_2 and V_3.

Figure 5. Moving average of the amplitude and the variance within the AE signal for a focus position of 15.010 *mm*

Figure 6. Bayesian classification of the focus position with respect to V_1, V_2, V_3.

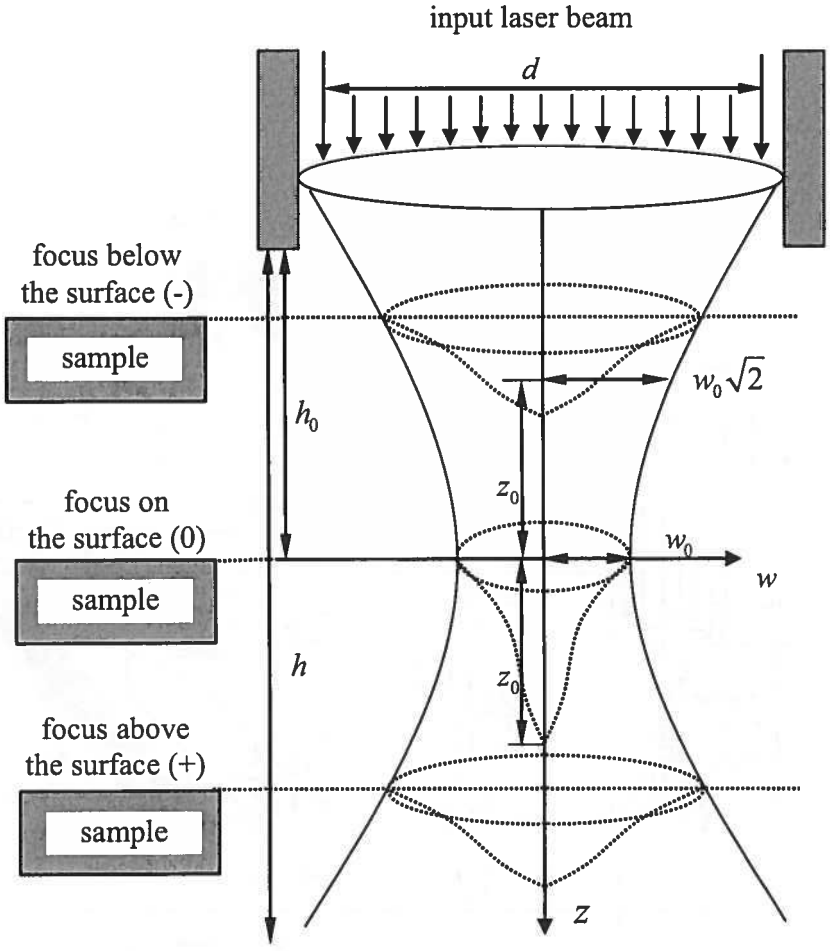

Figure 1. Geometry and profiles of the Gaussian laser beam.

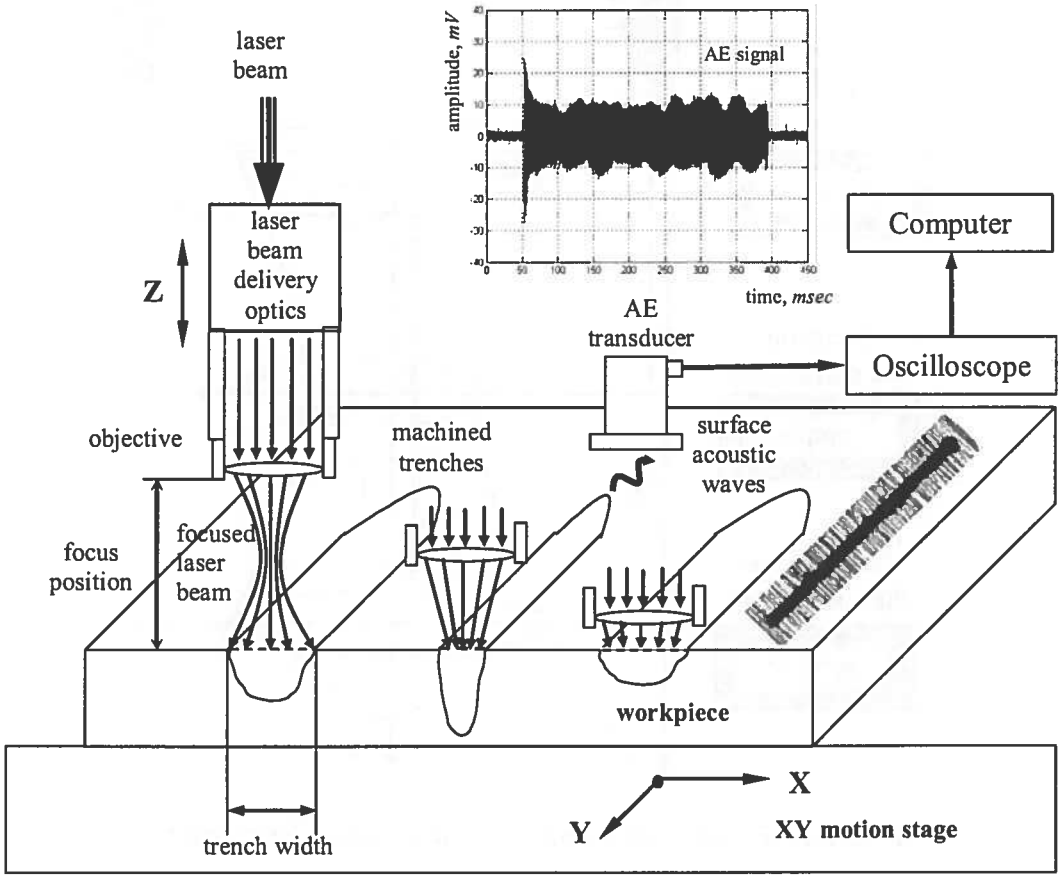

Figure 2. Schematics of the set-up and experiment.

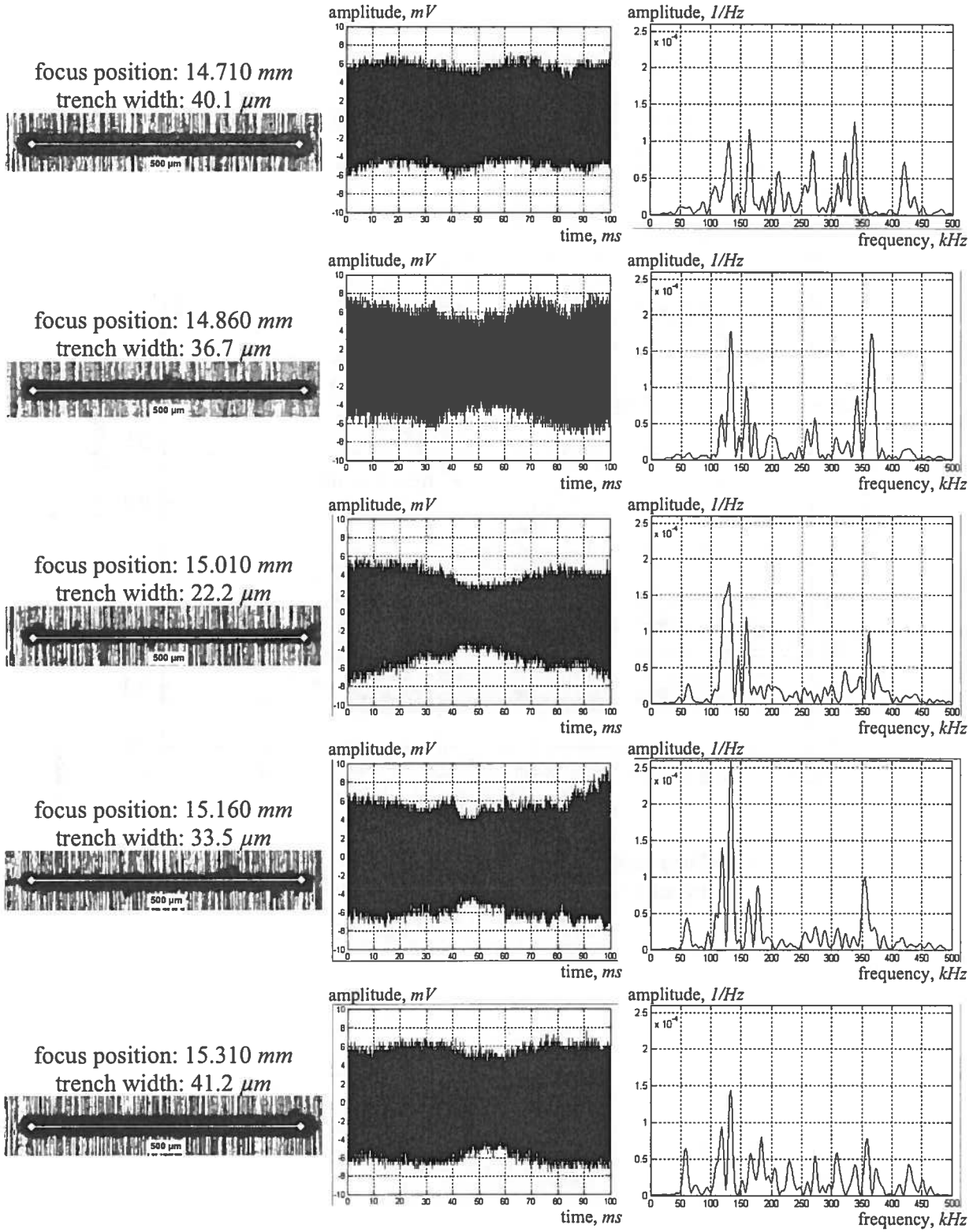

a) geometry of machined trenches b) measured AE signal b) power spectrum density

Figure 3. Examples of experimental data.

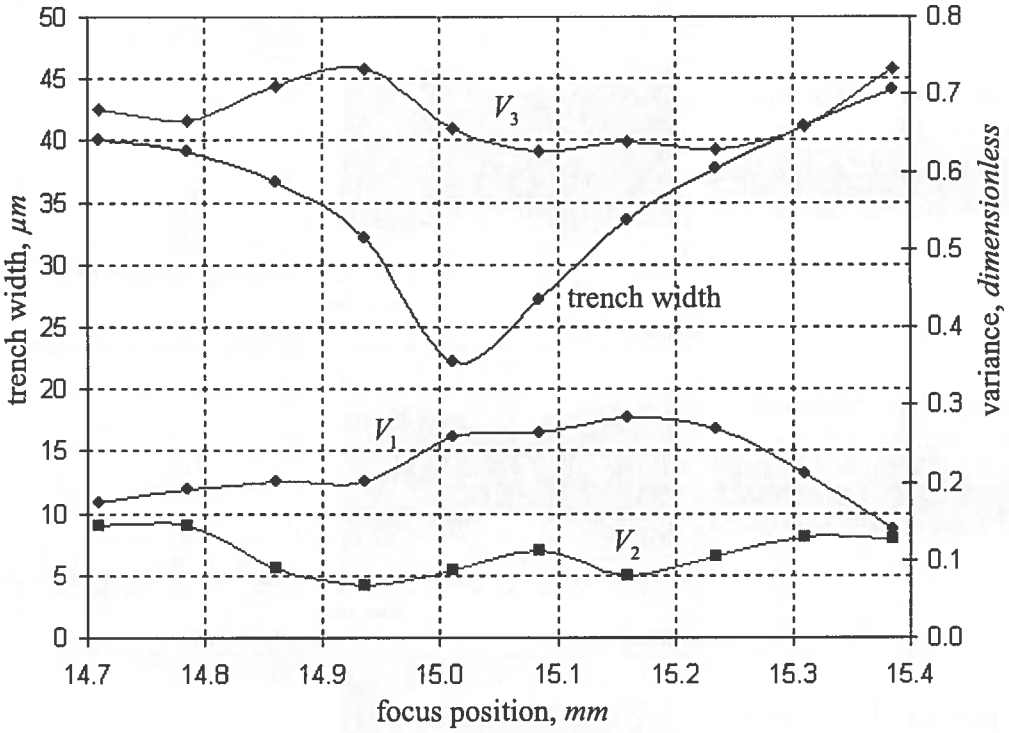

Figure 4. The relationships between the focus position, trench width and variances V_1, V_2 and V_3.

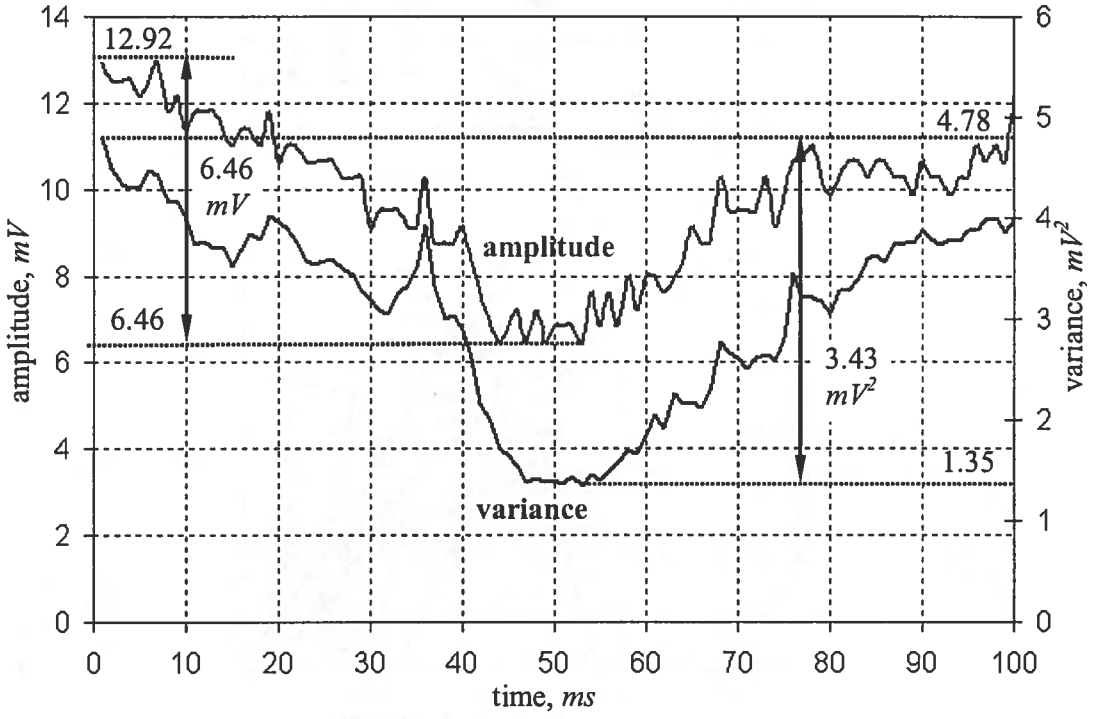

Figure 5. Moving average of the amplitude and the variance within the AE signal for a focus position of 15.010 *mm*

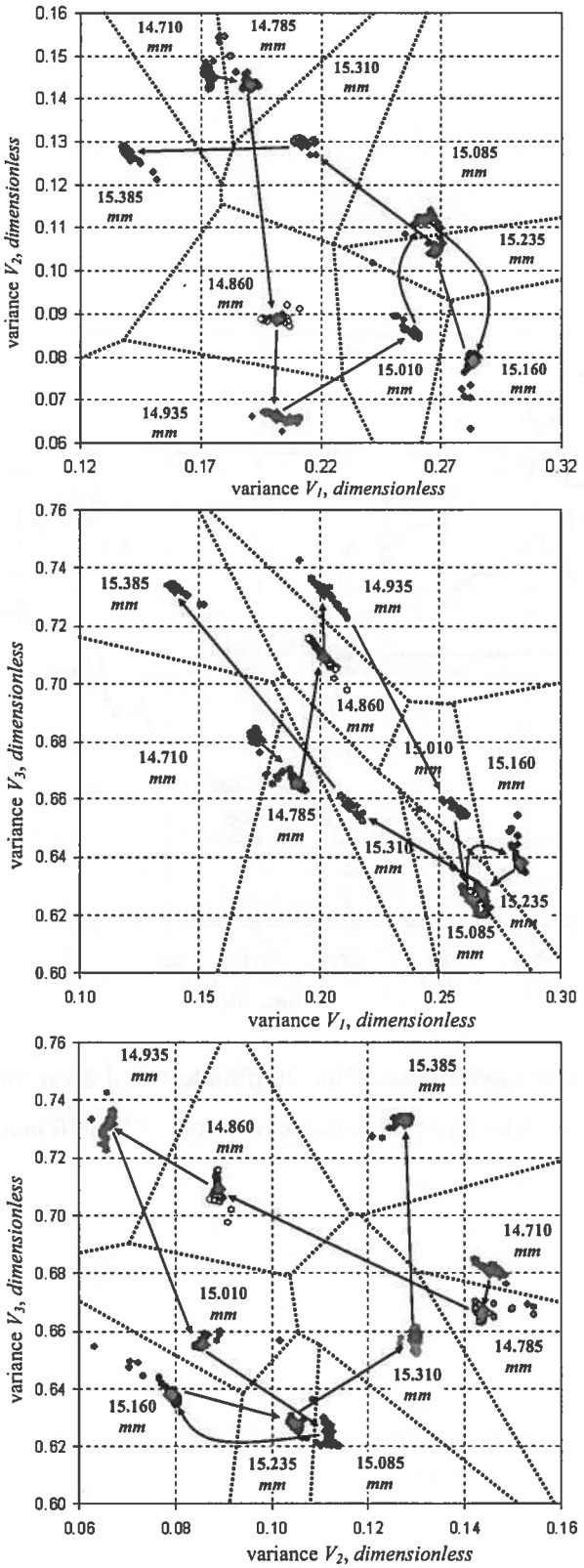

Figure 6. Bayesian classification of the focus position with respect to V_1, V_2, V_3.